symmetry

MDPI

Article

Organocatalytic Asymmetric Halocyclization of Allylic Amides to Chiral Oxazolines Using DTBM-SEGPHOS—Mechanistic Implications from Hammett Plots

Fotini Moschona, Christina Misirlaki, Nikolaos Karadimas, Maria Koutiva, Ioanna Savvopoulou and Gerasimos Rassias *

Department of Chemistry, University of Patras, 26504 Patra, Greece; fmoschona@windowslive.com (F.M.); up1057905@upnet.gr (C.M.); nick.m.karadimas@gmail.com (N.K.); up1061281@upnet.gr (M.K.); joanna_savv@hotmail.com (I.S.)

* Correspondence: rassiasg@upatras.gr

Abstract: The intramolecular halocyclization of alkenes possessing an internal heteroatom nucleophile leads to multifunctional heterocycles which are useful versatile intermediates in organic synthesis. The asymmetric chlorocyclisation of 2-substituted allylic amides gives access to chiral oxazolines bearing a chloromethyl moiety for further synthetic manipulation. The literature reports on this transformation involve complex syntheses of the 2-substituted allylic amides and cryogenic temperatures for achieving high enantioselectivities in the organocatalyzed halocyclization step. Based on the Heck reaction of aryl bromides and Boc-protected allylamine or allylamine benzamides, we developed a practical synthesis of 2-substituted allylic amides that does not require chromatography and accomplished their asymmetric halocyclization reaction with 24–92%ee under practical conditions (5 °C, CpME) catalyzed by (*S*)-(+)-DTBM-SEGPHOS. In addition, using appropriately substituted substrates, we generated Hammett plots and formulated a consistent mechanism for the halocyclization reaction which involves two competing modes of formation of the haliranium intermediate whose relative kinetics are governed by the electronic properties of the substrate.

Keywords: organocatalysis; halocyclization; 2-substituted allylic amides; 1,3-oxazolines; chiral diphosphines; Hammett plots

Citation: Moschona, F.; Misirlaki, C.; Karadimas, N.; Koutiva, M.; Savvopoulou, I.; Rassias, G. Organocatalytic Asymmetric Halocyclization of Allylic Amides to Chiral Oxazolines Using DTBM-SEGPHOS—Mechanistic Implications from Hammett Plots. *Symmetry* **2022**, *14*, 989. https://doi.org/10.3390/sym14050989

Academic Editor: Cosimo Cardellicchio

Received: 26 February 2022
Accepted: 10 May 2022
Published: 12 May 2022

1. Introduction

The halocyclization of alkenes with appropriate internal nucleophiles is a reaction of great interest as it provides diverse heterocyclic scaffolds that are components or synthetic intermediates in more complex molecules including pharmaceutically active agents [1–6].

Depending on the internal nucleophile, for example, carboxylic acid, alcohol or amide, the products can be halogenated lactones, ethers oxazolines or oxazine derivatives [7–9]. The reaction proceeds akin to the halogenation of alkenes, namely, via the formation of a haliranium ion followed by its ring opening by an S_N2 type reaction. Given any internal nucleophile, the haliranium intermediate may be ring opened by attack at either electrophilic carbon atom leading to the *exo-tet* and/or *endo-tet* cyclisation products. In case of intramolecular halocyclizations (Scheme 1), this reaction allows for construction of diverse heterocycles with concurrent incorporation of two heteroatoms across the C−C double bond generating one or two chiral centers in the process.

Consequently, substantial control of regio-, diastereo- and enantioselectivity is required otherwise a mixture of products will be formed. This challenge has been the focus of several reports in the literature where a number of chiral catalysts have been developed with varying degree of success depending on substrate type [10–14]. Halocyclization of allylic amides provides chiral oxazolines (or oxazines) which are key intermediates in the synthesis of organic compounds [1,15], natural products [16] and chiral ligands [17–19].

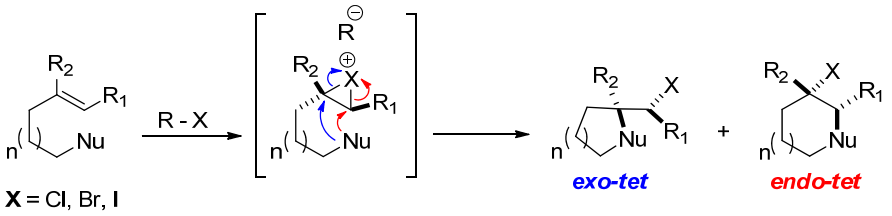

Scheme 1. Generic example of an intramolecular halocyclization reaction.

In connection with a program on the large-scale synthesis of a specific drug and analogues thereof, we identified chiral oxazolines as key intermediates in this effort and became interested in their synthesis via the asymmetric halocyclization of appropriate 2-substituted allylic amides.

Jaganathan et al. first reported the asymmetric chlorocyclization of 2-substituted2-substituted allylic amides with high enantioselectivity in the presence of $(DHQD)_2PHAL$ and dichlorodiphenylhydantoin (DCDPH) at −30 °C [20,21]. More recently, Kawato et al. reported high enantioselectivities in the analogous bromocyclization reaction of the same substrates using a chiral BINAP derivative and its mono-oxide [13,22]. However, in the above cases, extreme cryogenic temperatures were required in order to achieve high enantioselectivity (−78 °C, DCM) which are inappropriate for large scale synthesis. In addition, the synthesis of the allylic amides substrates in both of the protocols mentioned above, involve lengthy procedures and chromatographic purifications, also undesired in large scale syntheses.

In this work, we developed both a practical synthesis of 2-substituted allylic amides that does not require chromatography and a practical asymmetric halocyclization reaction of these substrates catalyzed by (*S*)-(+)-DTBM-SEGPHOS (Scheme 2). In addition, using appropriately substituted substrates we generated Hammet plots and formulated a mechanism for the halocyclization reaction that is consistent with our observations.

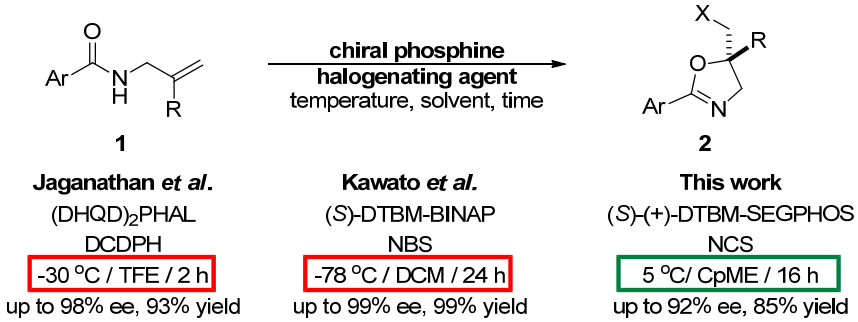

Scheme 2. Examples of asymmetric halocyclization of allylic amides to chiral oxazolines.

2. Results and Discussion

2.1. Synthesis of Substrates

Initially we decided to pursue a one-step synthesis of 2-substituted allylic benzamides (**3**, X = Ar^1, Route A, Scheme 3) through a Heck type reaction between benzamides of allylamine and arylbromides according to the protocol developed by Deng et al. for Boc-protected allylamine [23]. This method provided the desired products in good yields, but the regioselectivity for the 2-substituted isomer over the *trans* and *cis* topological isomers (resulting from Heck reaction at the terminal alkenyl carbon) was poor (Scheme 3, Route A). Consequently, we exploited Route B (**3**, X = O^tBu, Route B, Scheme 3) which involved the Heck reaction of the Boc-protected allylamine with aryl bromides according to the protocol of Deng et al. [23]. We found that the reported method is fully reliable and reproducible, allowing access to 2-substituted Heck products (**4**, Scheme 3) with good regioselectivity over the *trans* and *cis* topological isomers (9:1:1). Next, the crude Heck products were subjected to the standard Boc-deprotection conditions (TFA, DCM) but the isolated yields

of the corresponding allylic amines (**5**, Scheme 3) were very low. Following a short screen of alternative conditions, we found that treatment of the Boc-protected allylic amines with a slight excess methanesulfonic acid (1.1–1.5 eq) overnight at ambient conditions resulted in the complete and clean removal of the Boc group in a variety of solvents (DCM, MeCN, EtOAc). In most cases the mesylate salts of the allylic amines precipitated as crystalline solids from the reaction mixture and could be isolated via simple filtration although they contained similar levels of the respective cis and trans isomers. Pure 2-arylallylic amines were obtained by applying the standard amine work up extraction procedure with aqueous acid and base solutions which essentially eliminated the residual amounts of the *cis* and *trans* isomers.

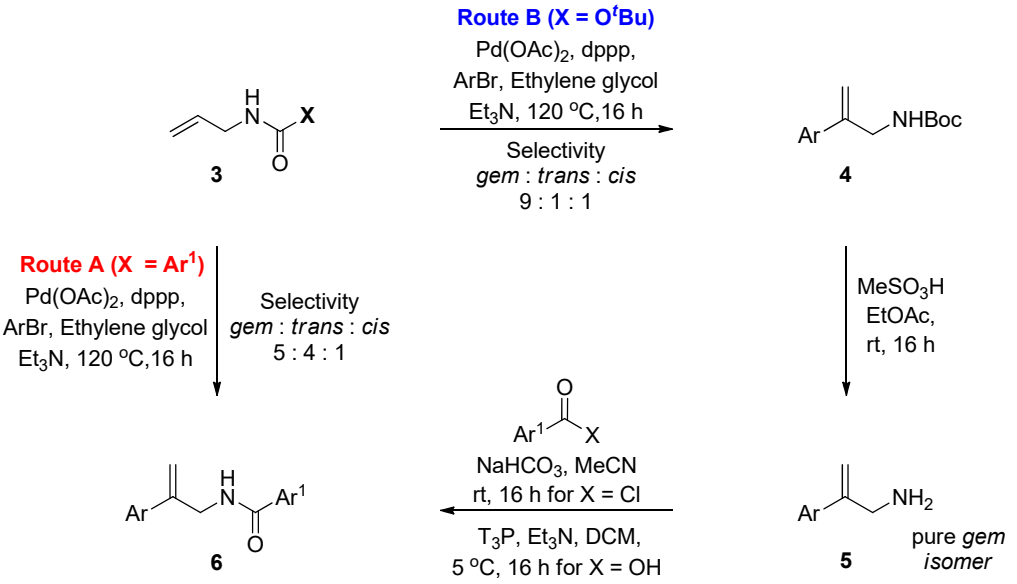

Scheme 3. Synthesis of 2-substituted allylic amides—substrates for halocyclization.

Finally, the 2-substituted allylic amides (**6**) were prepared from the allylic amines either via acylation with benzoylchlorides or by condensation with the corresponding benzoic acids activated by T_3P. In both cases, the products were isolated in very good yields (up to 80%) and excellent purity, and overall, the synthesis of desired substrates was achieved without need of chromatographical purifications.

2.2. Suppressing and Promoting the Racemic/Background Halocyclization Reaction

At the onset of any catalytic asymmetric reaction development, two sets of reaction conditions need to be established. The first relates to a procedure for efficiently generating the racemic products in order to develop a chiral HPLC or alternative analytical method for the determination of the enantiomeric ratio of the products subsequently obtained via asymmetric catalysis. The second set of conditions concerns the maximum suppression, ideally complete silencing of the background racemic reaction, thus ensuring that any conversion to the product (s) will arise exclusively from the chiral catalyst when this is added, hence the enantioselectivity and overall efficiency of the process is not compromised by alternative pathways.

In this context, a preliminary solvent screen revealed that the halocyclization reaction of **6e** (Scheme 4) with NBS and NCS was fast in relatively polar solvents such as DCM, EtOAc, THF, MeCN and MeOH but could be suppressed significantly in the less polar ethereal solvents such as CpMe and TBME. Consequently, we assessed the halocyclization reaction of **6e** with various halogenating agents at different temperatures in CpMe or TBME (Table 1). As mentioned earlier, our aim was to develop a halocyclization method that could operate at mild, non-cryogenic conditions, in order to be scale-up friendly; therefore, the temperature range studied was limited between ambient and −15 °C. After

16 h at this temperature range, NIS (*N*-iodosuccinimide), NBS (*N*-bromosuccinimide) and DCDMH (1,3-Dichloro-5,5-dimethylhydantoin) gave extensive conversions of the oxazoline product **7e** (Table 1, entries 1–4), meaning that a chiral catalyst of exceptional activity would be required to outcompete the generation of racemic product and preclude enantiomeric leakage.

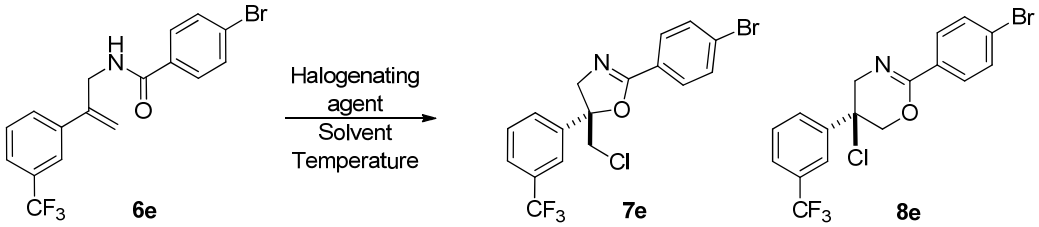

Scheme 4. The model halocyclization reaction used for establishing appropriate conditions.

Table 1. Halogenating agent and temperature screening.

Entry	Halogenating Agent	Solvent	Temperature (°C)	Conversion (16 h)
1	NIS	CpME	5	86%
2	NIS	CpME	−15	67%
3	NBS	CpME	5	92%
4	NBS	CpME	−15	88%
5	NCS	CpME	−15	6%
6	NCS	CpME	5	8%
7	NCS	EtOAc	rt	9%
8	NCS	TBME	−15	30% [1]
9	DCDMH	CpME	−15	89% [1]
10	NCS	EtOAc	5	99% [2]

[1] Mixture of 5-*exo* and 6-*endo* products; [2] In the presence of 20 mol% *rac* BINAP.

In contrast, NCS (*N*-chlorosuccinimide) reacted poorly with **6e** (<10% conversion) even at 5 °C after 16 h (Table 1, entries 5 and 6), thus providing an appropriate set of conditions to perform the catalytic asymmetric version of the reaction. Concerning the reparation of racemic **7e**, in order to develop a chiral HPLC method, we initially tested more polar solvents and the more reactive chlorinating agent DCDMH. Indeed, these modifications significantly promoted the chlorocyclisation process; this led to the formation of both *5-exo* (oxazoline) and *6-endo* (oxazine) cyclized products (Scheme 1), in a 3:1 and 4:1 ratio with DCDMH and NCS, respectively (determined by ^{1}H NMR). After testing several types of catalysts (protic acids, ureas, nucleophiles) we were able to achieve almost quantative formation of **7e** by inclusion of 20 mol% racemic BINAP into a set of reactions conditions that otherwise did not support the formation of **7e** (Table 1, entries 7 and 10). None of the alternative *6-endo* chlorocyclized product was observed in the reaction promoted by *rac*-BINAP.

2.3. Screening of Chiral Diphosphines as Organocatalysts

Having established both appropriate conditions to assess the catalytic asymmetric chlorocyclisation reaction of **6e** and the efficient and regioselective catalysis offered by *rac*-BINAP, we next screened a wide array of chiral diphosphines (Scheme 5).

These were tested at 10 mol% under the most practical conditions that suppressed the background reaction the most, namely NCS, CpME, 5 °C, 16 h and the reaction progress was monitored by HPLC. The results of catalyst screening are presented in Table 2.

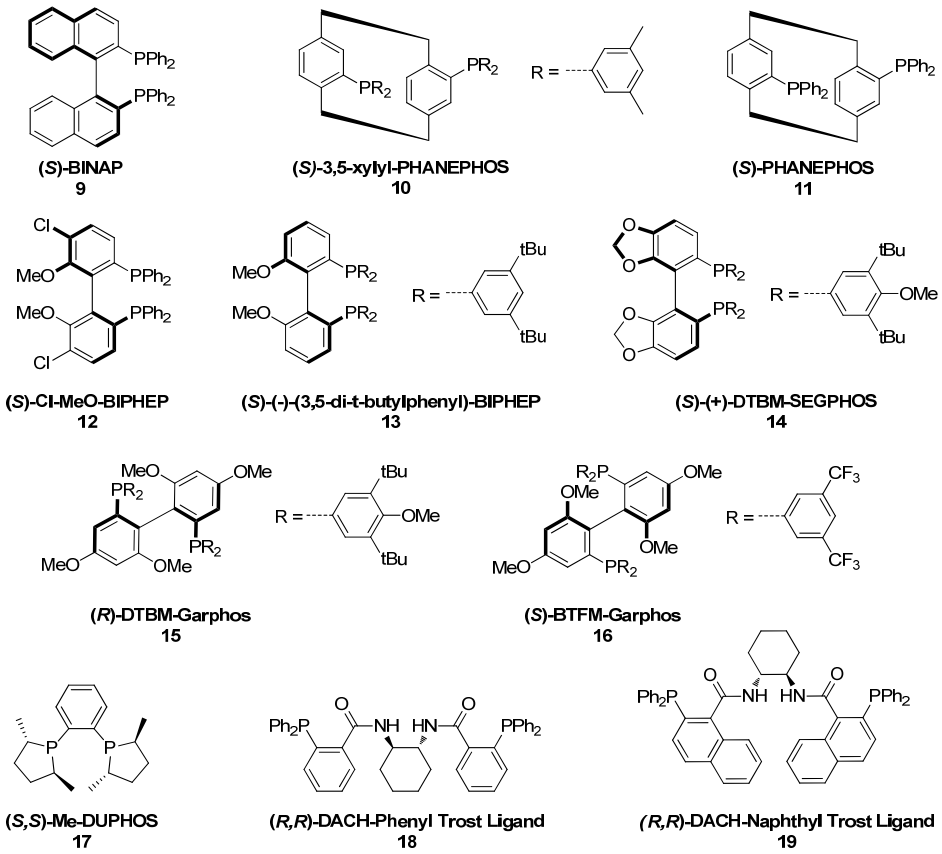

Scheme 5. Chiral diphosphines screened as catalysts in the asymmetric halocyclization reaction.

Table 2. Results from catalyst screening at 10 mol%. Conditions: **6e**, NCS, CpME, 5 °C, 16 h.

	Catalyst (10 mol%)	% Conversion (a/a by HPLC)	%ee
9	(*S*)-BINAP	96	27
10	(*S*)-3,5-xylyl-PHANEPHOS	85	<5
11	(*S*)-PHANEPHOS	96	<5
12	(*S*)-Cl-MeO-BIPHEP	8	<5
13	(*S*)-(-)-(3,5-di-t-butylphenyl)-BIPHEP	51	<5
14	(*S*)-(+)-DTBM-SEGPHOS	95	42
15	(*S*)-BTFM-Garphos	41	<5
16	(*R*)-DTBM-Garphos	48	<5
17	(*S*,*S*)-Me-DUPHOS	82	<5
18	(*R*,*R*)-DACH-Phenyl Trost Ligand	94	<5
19	(*R*,*R*)-DACH-Naphthyl Trost Ligand	78	<5

This screen exemplified that (*S*)-(+)-DTBM-SEGPHOS is the most competent catalyst among those tested for the chlorocyclisation reaction of **6e**, providing excellent conversion and appreciable enantioselectivity in the formation of **7e** (Table 2, catalyst 12). Interestingly, none of the other chiral phosphines, including those possessing high structural resemblance to DTBM-SEGPHOS, imparted meaningful enantioselectivity in the process. Conducting the (*S*)-(+)-DTBM-SEGPHOS-catalyzed reaction at lower temperature (−15 °C) led to the formation of **7e** with essentially the same %ee; hence, in all subsequent work, the reaction temperature was set at 5 °C.

2.4. Influence of the Amide Domain of the Substrate on Enantioselectivity

Having determined (*S*)-(+)-DTBM-SEGPHOS as the optimum catalyst, we next probed the influence of the substrate on the enantioselectivity of the process, starting from the

amide part of the structure. Towards this end, we generated a series of *p*-substituted benzamides (**6a**–**g**, Scheme 6) from the allylic amine bearing the *m*-CF_3-Ph substituent at the 2-position. As shown in Table 3, all substrates underwent the desirable halocyclization reaction in excellent yields and moderate enantioselectivity. Interestingly, the best enantioselectivity was obtained with the *p*-Me substituted benzamide, while all other more electron-withdrawing or -donating substituents on the benzamide moiety gave reduced enantioselectivity.

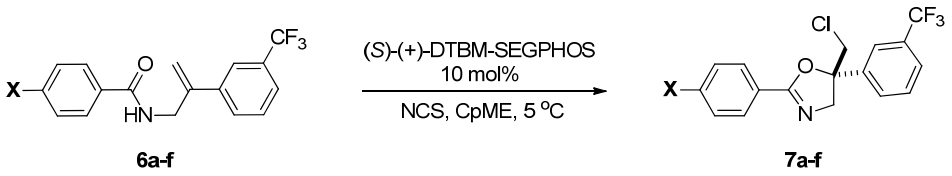

6a-f **7a-f**

Scheme 6. Investigation of benzamide *p*-substituent influence on enantioselectivity halocyclization.

Table 3. Results from benzamide *p*-substituent screening. Conditions: **6e**, NCS, CpME, 5 °C, 16 h.

Substrate	X	Hammett σ_p [24]	Regioselectivity 7:8 (%)	Yield (%) [a]	ee (%) [b]
6a	MeO	−0.27	97:3	95	50
6b	Me	−0.17	87:13	93	59
6c	H	0	97:3	95	48
6d	F	+0.06	90:10	94	44
6e	Br	+0.23	93:7	95	41.5
6f	CF_3	+0.54	97:3	86	36
6g	NO_2	+0.78	97:3	97	30

[a] Isolated yield. [b] Determined by chiral HPLC analysis.

In order to investigate further this unusual electronic effect on enantioselectivity we constructed the corresponding Hammett plot of %ee vs. σ_p constants for substrates **6a**–**g** (Figure 1). Standard Hammett plots involving rates of reactions are often linear with a positive slope (ρ value), suggesting that the reaction is promoted by electron-withdrawing groups and that built up of negative charge or destruction of a positive charge is involved in the rate determining step (RDS); a negative ρ value is indicative of the opposite effects. Nevertheless, there are many cases where Hammett plots are not linear, with "V" or inverted "V" trends being realized which signify a change in the RDS or switch to a different mechanism altogether. In this case, we observe an inverted "V"-shaped relationship between %ee and σ_p constants, which may be attributed to a change in either the enantiodetermining step along the same reaction mechanism or a change in mechanism.

The enantiodetermining step in this process concerns the installation of the halogen atom on the alkene namely the formation of the haliranium ion intermediate. The stereochemistry of the latter predetermines the stereochemistry of the halocyclization step as it is ring opened with inversion of configuration by the internal nucleophile: the amide carbonyl oxygen atom. Evidently, the electronic properties of the relatively distant amide carbonyl group significantly influence the asymmetric induction during the formation of the haliranium ion intermediate. In turn, the electronic properties of the benzamide group determine both the nucleophilicity of its oxygen atom and the pK_a of its N-H group, and these are governed to a significant extent by the *para* substituent of the benzamide ring. The reaction arguably commences with the formation of the new, chiral and more reactive than NCS chlorinating agent, namely, the chlorophosphonium species, resulting from reaction of the chiral phosphine with NCS (**20**, Scheme 7).

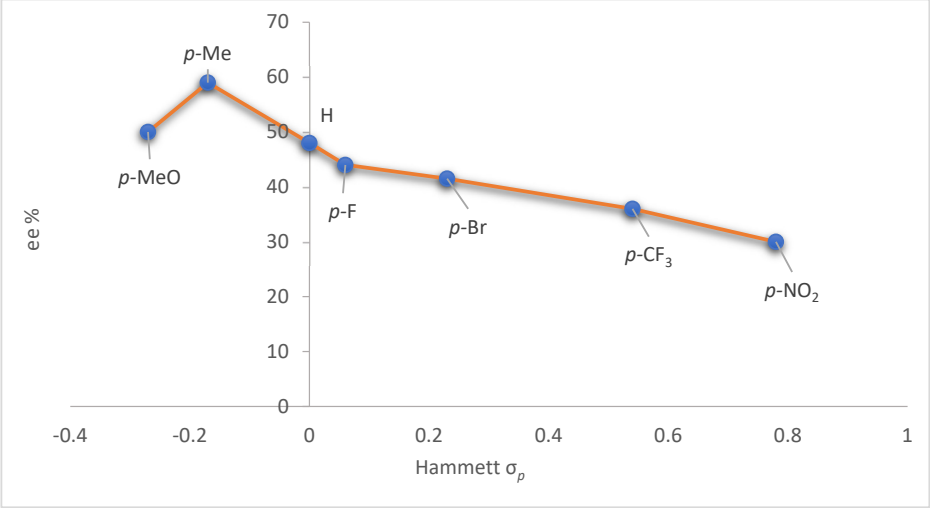

Figure 1. Hammett plot of benzamide *p*-substituent versus ee.

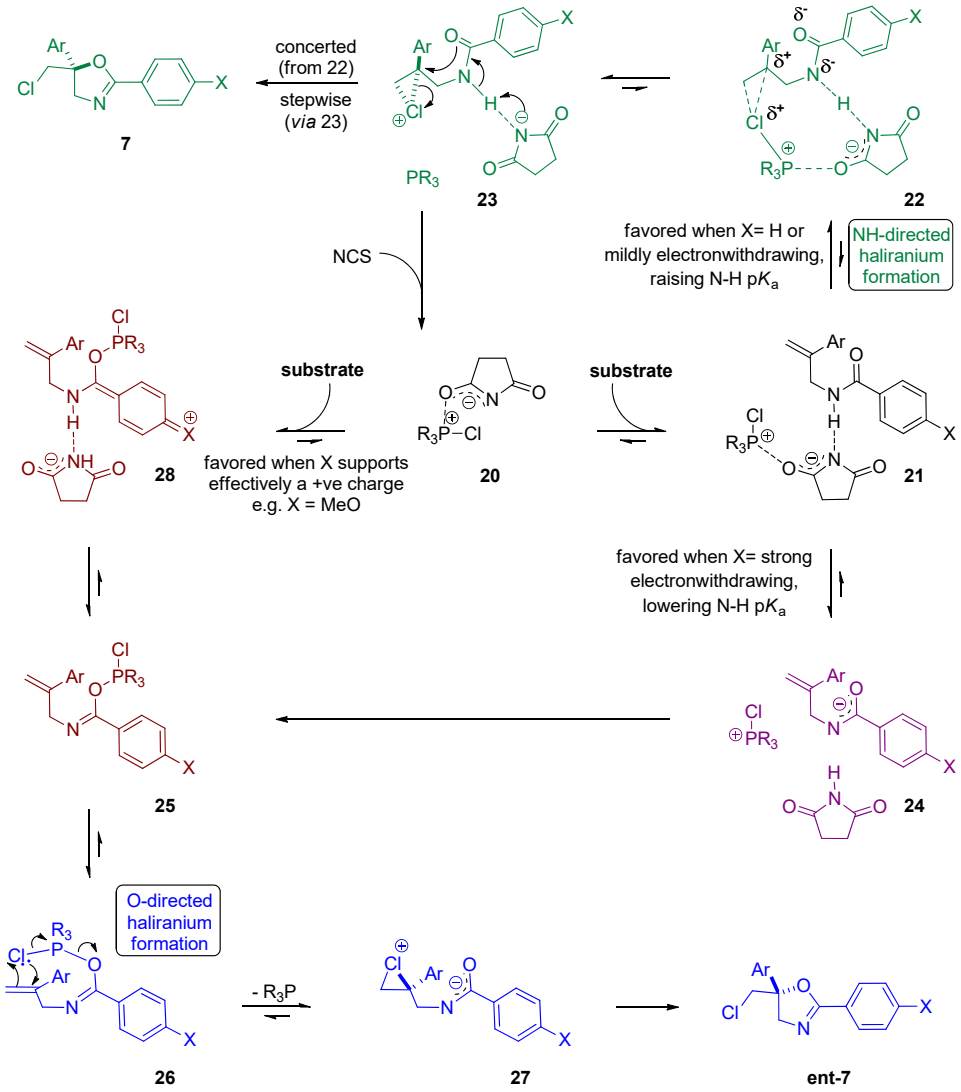

Scheme 7. Catalytic cycle and proposed pathways consistent with the Hammet plot in Figure 1.

In CpME, **20** is expected to exist as an intimate ion pair since non-polar solvents do not support charge separation and ion solvation. Equally, considering the optimum substrate **6b**, a hydrogen bonding interaction with **20** to form **21**, would also be favored in the non-polar reaction solvent, which in turn allows for the electrophilic chlorine atom to be positioned in the proximity of the alkene. This leads to complex and/or transition state **22**, where the chlorophoshonium cation, the succinimide anion and the substrate are held together in a highly organized assembly, thus facilitating the enantioselective transfer of the electrophilic chlorine atom to the alkene (NH-directed haliranium formation, Scheme 7). Complex/transition state **22** may convert to the product either directly, in a concerted fashion, or via the formation of the discreet chloriranium ion intermediate **23** (Scheme 7). As the electron-withdrawing capacity of the benzamide *p*-substituent increases, the pK_a of the amide proton decreases thus facilitating deprotonation of the substrate by the succinimide anion and establishment of an equilibrium between **21** and **24** (Scheme 7) [25]. The resulting anion **24** and its accompanying chlorophosphonium cation, as mentioned above, are expected not to exist as individually solvated ions in the non-polar solvent of the reaction (CpME) but rather combine towards a neutral species. Reaction of the amide anion via its oxygen atom on the positively charged phosphorous atom allows formation of adduct **25** (Scheme 7). In this adduct the electrophilic chlorine atom is favourably positioned in the vicinity of the alkene therefore supporting the generation of the chloriranium cation intermediate in an intramolecular fashion (**26**, O-directed haliranium formation, Scheme 7) with concomitant release of the chiral phosphine catalyst and the amide anion. The resulting zwitterion **27** is expected to cyclize fast in a 5-*exo-tet* manner (favored) to give the oxazoline product. We posit that the NH- and the O-directed haliranium formation modes generate preferentially chloriranium intermediates **23** and **26**, respectively, with opposite stereochemistries at the tertiary chlorine-bearing carbon atom, hence precipitating the opposite enantiomers of oxazolines **7**. Apparently, substrates with relatively nonacidic N-H, such as **6b**, support the NH-directed haliranium formation mode, which predominates on kinetic grounds (*ca* 4:1, hence *ca* 60%ee, assuming best case scenario of complete enantioselectivity from each transition state) over the O-directed haliranium formation mode, presumably responsible for favoring mostly the opposite enantiomer. Substrates with increasingly more acidic N-H support better its abstraction by the succinimide anion, and consequently the O-directed haliranium formation mode gains ground thus leading to decreased enantioselectivity. Nevertheless, the NH-directed haliranium formation mode appears to be the dominant reaction pathway, since the O-directed haliranium formation mode cannot prevail even with its best advocate, substrate **6g** (NH/O directed ca 1.85:1, hence ca 30%ee). On the other end of the spectrum, with substrate **6a**, despite the *p*-MeO substituent which renders its N-H bond the least acidic among those examined, hence more supportive of the NH-directed haliranium formation mode, slightly lower enantioselectivity is obtained in comparison with **6b**. Additionally, in this case, we believe the enantioselectivity leakage occurs through an increased contribution from the O-directed mode of haliranium formation (NH/O directed ca 3:1, hence ca 50%ee). The rationale for this is based on the substantially increased Lewis basic/nucleophilic character of the amide carbonyl oxygen in substrate **6a**, due to the *p*-MeO substituent. In this case, the electronically enhanced and nucleophilic carbonyl is expected, to a certain extent, to attack the phosphorous atom in the chlorophoshonium salt with the amide portion becoming positively charged in the process. The succinimide anion displaced from **20** may now attract more efficiently the N-H of the positively charged amide, thus giving rise to adduct **28** (Scheme 7). This N-H proton in this positively charged species is much more acidic than that in the corresponding neutral complex **21** (even when X = NO_2); therefore, complete deprotonation by the succinimide anion to give adduct **25** is much more favored. Overall, an alternative sequence of reactions is realized that also leads to the O-directed haliranium formation (**26**, Scheme 7). The difference between the strongly donating and strongly withdrawing *p*-substituents in the benzamide domain, is that with the former the P-O bond is formed first followed by deprotonation, whereas with the latter, deprotonation precedes

the formation of the P-O bond. Overall, we posit that the inverted "V" shape in the %ee vs. σ_p Hammett plot arises from two competing modes of formation of the haliranium intermediate (NH- or O-directed) each leading to the product with opposite enantioselectivities. The asymmetric halocyclization reaction of all *p*-substituted benzamides tested appears to proceed via both mechanisms, albeit at different rates. One mechanism is more favored strongly by resonance electron-donating groups and electron-withdrawing groups (substituents with large negative or positive values of σ_p Hammet constants, respectively), while the alternative mechanism is more favored by electron neutral groups (σ_p Hammet constants close to zero). In both modes of haliranium ion formation proposed, the amide group bridges the alkene and the halogenating agent, which is consistent with the observed influence of the remote amide group on enantioselectivity. Furthermore, the proposed modes of reactions are also consistent with the %ee pattern observed with varying the electronic properties of the benzamide group.

2.5. Influence of the Aryl Substituent in the Alkene Domain

Next, we decided to investigate how the enantioselectivity of the reaction is influenced by the electronic properties of the alkene, which in turn are largely governed by the aryl substituent at the 2-position. The Heck reaction in our substrate synthesis allowed for the introduction of several *p*-substituted phenyl groups, intended to support the construction of a Hammett plot. The Heck reaction was not successful in installing the *p*-MeO- and *p*-Me-phenyl groups; however, we did not consider this as a major setback for the study for the following reason. Electron rich substituents on the alkene force the ring opening of the corresponding haliranium intermediates generating a stabilized benzylic cation, which is attacked by the nucleophile (internal or external) via an S_N1 mechanism at either side thus precluding high enantioselectivity (Scheme 8). In the asymmetric halocyclization of 2-substituted amides reported independently by Jaganathan et al. and Hamashima et al., the 2-(*p*-MeO)-phenyl substrate gave 20 and 7%ee, respectively; this was a substantial deviation from other substrates (85–99%ee) [13,21].

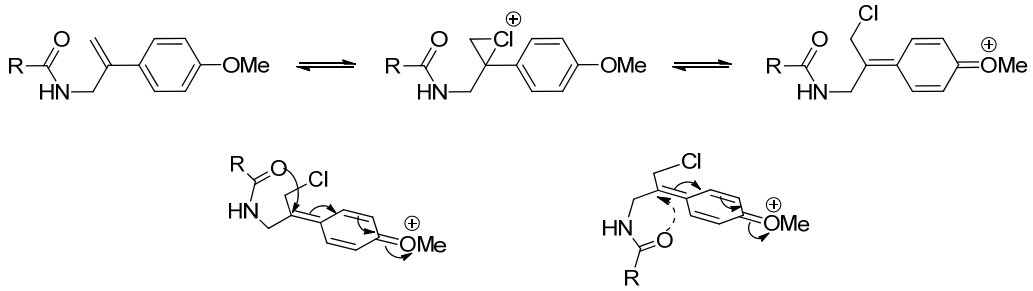

Scheme 8. Assessing the impact of aryl alkene *p*-substituent on halocyclization enantioselectivity.

Following the Heck reaction of Boc-protected allylic amine with various *p*-substituted aryl bromides and Boc deprotection, all allylic amines (**5**, Scheme 3) were converted to the corresponding benzamides (**6h–l**, Table 4) and subjected to the (*S*)-(+)-DTBM-SEGPHOS-catalyzed halocyclization reaction under the same conditions (Scheme 9). All substrates were converted to the corresponding chiral oxazolines in good to excellent yields and, in most cases, with significant enantioselectivity.

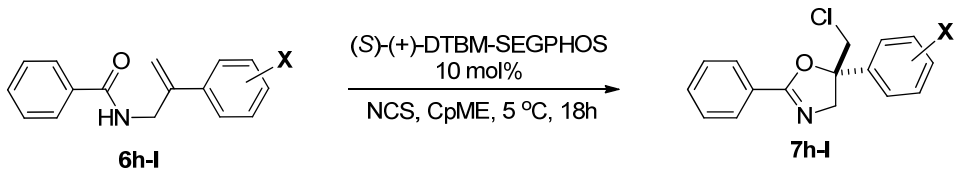

Scheme 9. Assessing the impact of aryl alkene *p*-substituent on the halocyclization ee.

Table 4. Results from different *p*-substituted phenyl groups on the alkene domain.

Substrate	X	Hammett σ_p	Regioselectivity 7:8 (%)	Yield (%) [a]	ee (%) [b]
6h	H	0	**93:7**	99	65
6i	*p*-F	+0.06	**91:9**	91	68
6j	*p*-CONH^{i}Bu	+0.36	**87:13**	70	80
6k	*p*-CF_3	+0.54	**97:3**	98	60
6l	*p*-CN	+0.66	**97:3**	60	20

[a] Isolated yield. [b] Determined by chiral HPLC analysis.

In this series, the pattern observed in the Hammett plot of %ee vs. σ_p constants of the 2-(*p*-substituted)-phenyl allylic benzamides, is also an inverted "V" shape signifying a change in the enantiodetermining step, depending on the electronic properties of the alkene domain. More specifically, starting from the electronically neutral, on relative terms, phenyl substituted alkene **6h** (X = H, Table 4, Figure 2) and, moving gradually to electron-withdrawing X groups such as **6j** (X = CONH^{i}Bu, Table 4, Figure 2), an increase in enantioselectivity is observed, whereas installation of stronger electron-withdrawing X groups as in **6l** (X = CN, Table 4, Figure 2), leads to considerable attenuation of enantioselectivity.

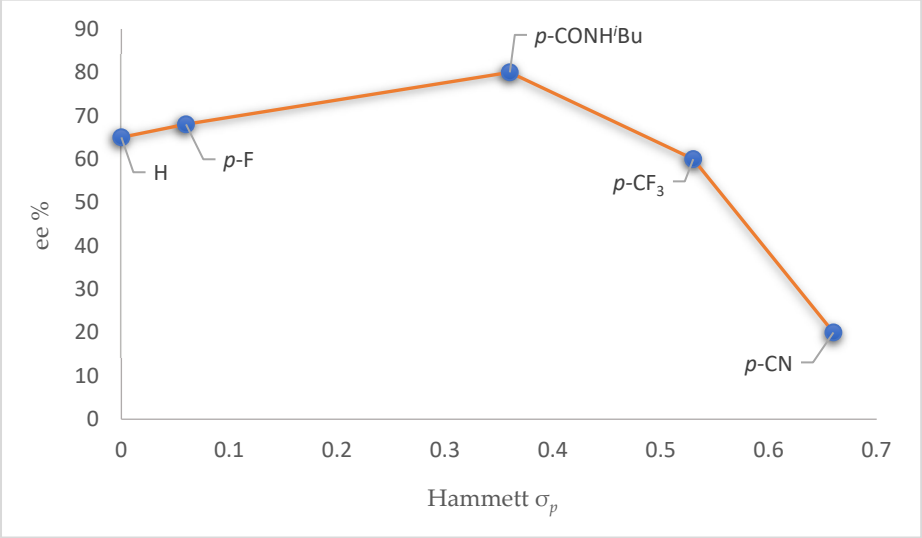

Figure 2. Hammett plot of the *p*-substituted phenyl groups on the alkene domain versus ee.

We believe the negative ρ value in the latter part of the plot is attributed to the low reactivity/nucleophilicity of this type of alkene substrates which are reluctant to develop strong interactions with the chiral halogenating species leading to complex **22** (Schemes 7 and 10). The less the alkenyl domain interacts with the electrophilic chlorine atom, the freer it is to rotate along the single bonds of the allylic part, thus exposing equally either alkene side to the halogenating agent. Consequently, due to the essentially intramolecular nature of the halogen atom transfer to the alkene (enantiodetermining step), eventual reaction would give the two enantiomeric chloriranium ions with low enantioselectivity. The resulting poorly stabilised chloriranium ions **(*S*/*R*)-29/P*** (Scheme 10) are expected to be attacked rapidly by the carbonyl group and give the oxazoline products **(*S*/*R*)-7** (Scheme 10). The opposite effect is expected with X-substituents with σ_p constants closer to zero such as **6h** (X = H) and **6i** (X = F), which render the alkene domain more nucleophilic. In this case, strong interactions with the chiral halogenating species ensue, leading to complex **23** (Scheme 7), where the chiral chlorophosphonium moiety may determine the reacting alkene rotamer and facial selectivity.

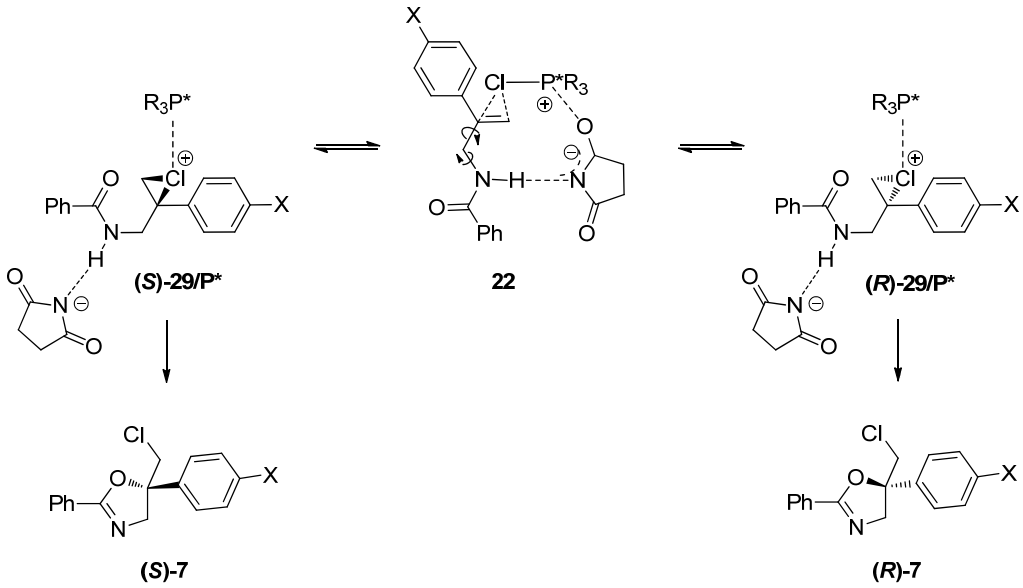

Scheme 10. Assessing the impact of aryl alkene *p*-substituent on the halocyclization %ee.

It is well established that in the reaction between an alkene and various electrophilic halogenating species, the initial halogen transfer that forms the haliranium intermediate is a reversible process [26]. The resulting chloriranium complexes **(*S*/*R*)-29/P*** (Scheme 10) for X = H, F are much more stable in comparison to those generated from the other substrates tested (X = CONH^{i}Bu, CF_3, NO_2), hence less prone to give the reverse reaction and instead cyclise to **(*S*/*R*)-7** shedding their charged character. Consequently, the product enantioselectivity in this case reflects that of the kinetic preference of chiral complex **22** in transferring the halogen to the *pro-R* or *pro-S* faces of the alkene. Gradual destabilization of choriranium ions in complexes **(*S*/*R*)-29/P***, by subtle increases in the σ_p constant of the X substituent (Table 4), reaches a point where the reverse process, namely, the retraction of the halogen atom by the phosphine, becomes favorable thus establishing an equilibrium between **22** and complexes **(*S*/*R*)-29/P***. In turn, this allows some degree of thermodynamic control in the formation of **(*S*/*R*)-29/P*** complexes and therefore a potential increase/correction of selectivity, rather than exclusive kinetic control. Nevertheless, it is unclear whether this equilibrium increases the population of the most stable **29/P***complex (matched case), leading to the major oxazoline enantiomer or engages/traps the most stable **29/P*** for longer in the equilibrium process, thus allowing the least stable **29/P*** complex (mismatched case) to cyclize and precipitate the major oxazoline enantiomer.

2.6. Investigation of Substrate Scope

Next, we synthesized and tested more substrates in our (*S*)-(+)-DTBM-SEGPHOS-catalyzed halocyclization reaction (Scheme 11). Interestingly all *meta*-substituted phenyl alkene substrates gave the corresponding oxazolines **7m**, **7n** and **7c** with essentially the same enantioselectivity 48–52%ee. This result is consistent with our mechanistic understanding, since *meta* substituents only exert a small inductive effect on the aryl alkene domain in contrast to the strong resonance effects, hence significant influence on enantioselectivity observed with their *para*-substituted counterparts. Along the same lines, the *p*-sulfonamide oxazoline product **7o** was obtained with poor enantioselectivity (26%ee), and this is consistent with the strong electron withdrawing capacity of the sulfonamide group (σ+ constant +0.65) and mirrors the result of the *p*-CN derivative (σ+ constant +0.65, 20%ee). 1-Naphthlyl oxazoline **7p** was obtained with 36%ee, and this is attributed to enantioselectivity leakage through the mechanism describe in Scheme 8, since the naphthyl ring is a particularly good electron donor due to the reduced aromatic character of one of its benzene rings. This attribute is absent from the electron deficient 3-pyridyl and 6-quinolinyl

derivatives, which gave the highest enantioselectivities in this series of substrates (76 and 88%ee, respectively).

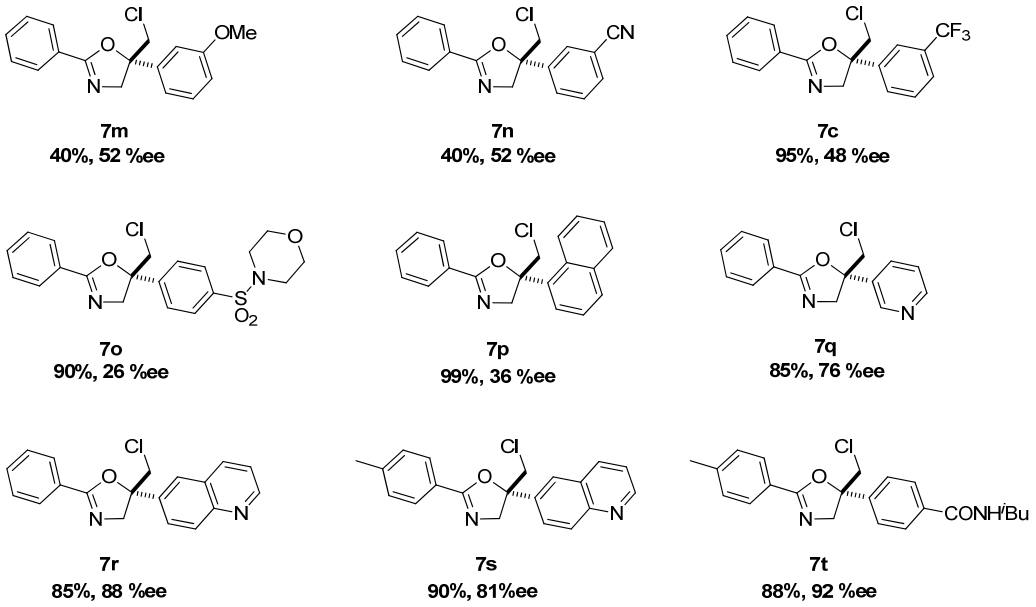

Scheme 11. Structures, yields and ees of chiral oxazolines obtained with additional substrates.

Finally, we tested substrates that possess the optimum benzamide and aryl domains for enantioselectivity, in order to assess if their effects are additive. Indeed, oxazolines **7s** and **7t** were obtained with higher enantioselectivities (81 and 92%ee, respectively, Scheme 11) than the corresponding analogues bearing only one of the optimum substituents (88 and 80%ee for **7r** and **7j**, respectively).

3. Conclusions

We developed an enantioselective chlorocyclization reaction of -2-substituted allylic amides using (*S*)-(+)-DTBM-SEGPHOS as the chiral organocatalyst. Our process is the third reported in this context and complements those previously reported with DTBM-BINAP and $(DHQD)_2PHAL$, and it is more suitable for large scale syntheses. More specifically, we have developed a much simpler and practical synthesis of the alkene substrates in one or three steps, without need for chromatography and conditions that allow the halocyclization process to proceed at 5 °C rather than at cryogenic temperatures, affording chiral oxazolines typically at >85% yield and up to 94%ee. Furthermore, we pursued a systematic study of appropriately substituted substrates that enabled the construction of Hammett plots and provided an increased understanding on the catalytic cycle and the reaction pathways that govern the enantioselectivity of the process. The encouraging results and insight gained from this work have triggered further studies in our group concerning the organocatalyzed asymmetric halocyclization of other substrates such as alkenyl alcohols, carbamates and amines and results from these investigations will be reported in due course.

4. Materials and Methods

4.1. Chemistry Materials and Instrumentation

All reagents and solvents were obtained from commercial sources and used without further purification unless otherwise stated. ^1H and ^{13}C NMR spectra were recorded on Bruker spectrometers at 400 or 600 MHz and 101 or 151 MHz, respectively. Chemical shifts were reported on δ scale in ppm with the solvent indicated as the internal reference. Coupling constants were reported in Hertz (Hz) and the standard abbreviations indicating multiplicity were used as follows: s = singlet, s (br) = broad singlet, d = doublet, t = triplet, q = quartet, and m = multiplet. High resolution mass spectrometry (HRMS) experiments

were recorded with electrospray ionization (ESI) on a Synapt G2-Si mass spectrometer. The purity of all final compounds was confirmed to be ≥95% by NMR and/or HPLC using Agilent 1100 with the UV detector set at 220 nm, equipped with a Phenomenex Luna column (50 × 3.0 mm, 2.6 μm) at 40 °C, at a flow rate of 1.0 mL/min and solvent gradient of 7 to 95% B over 5.5 min, followed by 0.5 min at 95% B, followed by gradient change to 7% B over 2 min: solvent A = 0.05% TFA in water; solvent B = 0.05% TFA in acetonitrile. NMR spectra for intermediates and final products including chiral HPLC methods, are provided in the Supplementary Material.

4.2. Experimental Procedures

4.2.1. General Procedure for the Gem-Selective Heck Reaction

Tert-butyl allylcarbamate (3.18 mmol, 1 eq), aryl bromide (3.82 mmol, 1.2 eq), palladium (II) acetate (3 mol%), 1,3-bis(diphenylphosphino)propane (6 mol%) and degassed ethylene glycol (0.42 M) were charged in an oven-dried 100 mL round-bottom flask equipped with a magnetic stir bar and an argon atmosphere was established. Triethylamine (6.36 mmol, 2 eq) was added under N_2. The reaction mixture was stirred at 115 °C for 16 h and monitored by HPLC. At completion, the solution was cooled at room temperature and water (75 mL) was added. The aqueous phase was extracted with EtOAc (3 × 15 mL). The organic phases were combined and washed with HCl 0.1 M (2 × 12 mL), 5% $NaHCO_3$ (1 × 12 mL) and brine (1 × 12 mL). The organic phase was separated and dried over Na_2SO_4. Charcoal (150 mg) was added in the organic phase and the mixture was stirred at 60 °C for 2 h. After filtration though diatomaceous earth, the solvent was removed under reduced pressure to afford an oil which was used in the next step without further purification.

4.2.2. General Procedure for Boc Deprotection

Crude *N*-Boc-2-arylallylamine (1 eq) was added in a round-bottom flask equipped with magnetic stir bar and dissolved in EtOAc (0.56 M). Methanesulfonic acid (1.2 eq) was added in the flask. The reaction was stirred for 16 h at room temperature and monitored by HPLC. The solvent was removed under reduced pressure and the residue was dissolved in TBME (0.35 M). The organic phase was extracted with 1 M HCl (×3). The aqueous phases were combined, and the pH was adjusted to 11–12. The aqueous phase was then extracted with DCM (×3). The organic phases were combined and dried over Na_2SO_4. The solvent was removed under reduced pressure to afford the pure amine.

4.2.3. General Procedure for Amide Formation Using Acyl Chlorides

In a round-bottom flask equipped with magnetic stir bar, the arylallylamine (1 eq) was dissolved in MeCN (0.08 M). $NaHCO_3$ (1.3 eq) and benzyl chloride (1 eq) were added. The reaction was stirred for 16 h at room temperature and monitored by HPLC. The solvent was removed under reduced pressure and the crude was dissolved in TBME. The organic phase was washed with HCl 0.1 M (×2), 5% $NaHCO_3$ and brine. The organic phase was dried over Na_2SO_4 and the solvent was removed under reduced pressure to afford an oil residue.

4.2.4. General Procedure for Amide Formation Using Carboxylic Acids

Amine (1.1 eq), carboxylic acid (1 eq) and triethylamine (7.5 eq) were dissolved in DCM (0.6 M) in a round-bottom flask equipped with magnetic stir bar. The mixture was stirred for 15 min at −15 °C. T_3P (1.7 eq) was dissolved in DCM (1.81 M) and added in the flask at 3 portions during 1 h. The mixture was stirred at 4 °C for 16 h and monitored by HPLC. At completion, the reaction mixture was washed with HCl 0.1 M (×2), 5% $NaHCO_3$ and brine. The organic phase was dried over Na_2SO_4. The solvent was removed under reduced pressure to afford a solid.

4.2.5. General Procedure for Racemic Halocyclization and Oxazolines

In an oven-dried vial equipped with magnetic stir bar, benzamide (1 eq) was dissolved in EtOAc (0.29 M). *rac*-BINAP was added (20 mol%) under N_2 atmosphere and the mixture was stirred at 4 °C for 15–20 min. Next, NCS (1.6 eq) was added under N_2 atmosphere and the reaction mixture was stirred at 4 °C for 16 h and monitored by HPLC. At completion, the organic phase was washed with NaOH 0.2 M (×2), deionized water and brine. The organic phase was dried over Na_2SO_4 and the solvent was removed under reduced pressure to afford an oil. Analytically pure samples for developing the chiral HPLC methods were obtained by column chromatography.

4.2.6. General Procedure for the Asymmetric Halocyclization Reaction

The unsaturated amide (1 eq) was dissolved in anhydrous CpME (0.29 M) in an oven-dried vial equipped with magnetic stir bar. (*S*)-DTBM-SEGPHOS were added (10 mol%) under N_2 atmosphere. The mixture was stirred at 4 °C for 15–20 min and NCS (1.3 eq) was added to the vial under N_2 atmosphere. The reaction mixture was stirred for 16 h at 4 °C and monitored by HPLC. At completion, the organic phase was washed with NaOH 0.2 M (×2), deionized water and brine. The organic phase was dried over Na_2SO_4 and the solvent was removed under reduced pressure to afford an oil residue. Analytically pure samples were obtained by column chromatography, although the crude product is of appropriate quality to be used for the determination of %ee or further transformations.

Supplementary Materials: The following are available online at https://www.mdpi.com/article/10.3390/sym14050989/s1, NMR and chiral HPLC data.

Author Contributions: Conceptualization, G.R.; methodology, G.R., F.M., C.M. and I.S.; software, F.M.; validation, F.M., C.M. and I.S.; formal analysis, F.M., C.M., N.K. and I.S.; investigation, F.M., C.M., N.K., M.K. and I.S.; resources, G.R.; data curation, F.M., C.M., N.K. and I.S.; writing—original draft preparation, G.R.; writing—review and editing, G.R. and F.M.; visualization, N.K. and M.K.; supervision, G.R. and F.M.; project administration, G.R. and F.M.; funding acquisition, G.R. All authors have read and agreed to the published version of the manuscript.

Funding: This research received no external funding.

Institutional Review Board Statement: Not applicable.

Informed Consent Statement: Not applicable.

Data Availability Statement: Not applicable.

Acknowledgments: The early work conducted by the undergraduate students Maria Tereza Hatzinaki, Dionysia Rigopoulou and Vasilios Sakellaropoulos on the synthesis of substrates and screening of various types of catalysts is greatly acknowledged. We would also like to acknowledge the staff of the Laboratory of Instrumental Analysis of the Faculty of Science involved in the acquisition of NMR and mass spectra.

Conflicts of Interest: The authors declare no conflict of interest.

References

1. Tahir, S.K.; Nukkala, M.A.; Zielinski Mozny, N.A.; Credo, R.B.; Warner, R.B.; Li, Q.; Woods, K.W.; Claiborne, A.; Gwaltney, S.L., 2nd; Frost, D.J.; et al. Biological activity of A-289099: An orally active tubulin-binding indolyloxazoline deriivative. *Mol. Cancer Ther.* **2003**, *2*, 227–233. [PubMed]
2. Rastelli, E.J.; Coltart, D.M. Asymmetric synthesis of (+)-*anti*- and (-)-*syn*-mefloquine hydrochloride. *J. Org. Chem.* **2016**, *81*, 9567–9575. [CrossRef] [PubMed]
3. Gorter de Vries, R.J.; Lafont, S.; de Saint, M.G.; Kozlovic, S. Crystalline Forms of (s)-Afoxolaner. WO 2018187623A1, 26 May 2020.
4. Feng, X.; Jiang, G.; Xia, Z.; Hu, J.; Wan, X.; Gao, J.M.; Lai, Y.; Xie, W. Total synthesis of (-)-conolutinine. *Org. Lett.* **2015**, *17*, 4428–4431. [CrossRef] [PubMed]
5. Yan, J.; Zhou, Z.; He, Q.; Chen, G.; Wei, H.; Xie, W. The applications of catalytic asymmetric halocyclization in natural product synthesis. *Org. Chem. Front.* **2022**, *9*, 499–516. [CrossRef]

6. Xie, W.; Jiang, G.; Liu, H.; Hu, J.; Pan, X.; Zhang, H.; Wan, X.; Lai, Y.; Ma, D. Highly enantioselective bromocyclization of tryptamines and Its application in the synthesis of (-)-chimonanthine. *Angew. Chem. Int. Ed. Engl.* **2013**, *125*, 13162–13165. [CrossRef]
7. Castellanos, A.; Fletcher, S.P. Current methods for asymmetric halogenation of olefins. *Chem. Eur. J.* **2011**, *17*, 5766–5776. [CrossRef]
8. China, H.; Kumar, R.; Kikushima, K.; Dohi, T. Halogen-induced controllable cyclizations as diverse heterocycle synthetic strategy. *Molecules* **2020**, *25*, 6007. [CrossRef]
9. Denmark, S.E.; Kuester, W.E.; Burk, M.T. Catalytic, asymmetric halofunctionalization of alkenes—A critical perspective. *Angew. Chem. Int. Ed. Engl.* **2012**, *51*, 10938–10953. [CrossRef]
10. Veitch, G.E.; Jacobsen, E.N. Tertiary Aminourea-catalyzed enantioselective iodolactonization. *Angew. Chem. Int. Ed. Engl.* **2010**, *112*, 7490–7493. [CrossRef]
11. Denmark, S.E.; Burk, M.T. Enantioselective bromocycloetherification by Lewis base/chiral Bronsted acid cooperative catalysis. *Org. Lett.* **2012**, *14*, 256–259. [CrossRef]
12. Cheng, Y.A.; Yu, W.Z.; Yeung, Y.-Y. Carbamate-catalyzed enantioselective bromolactamization. *Angew. Chem. Int. Ed. Engl.* **2015**, *127*, 12270–12274. [CrossRef]
13. Kawato, Y.; Kubota, A.; Ono, H.; Egami, H.; Hamashima, Y. Enantioselective bromocyclization of allylic amides catalyzed by BINAP derivatives. *Org. Lett.* **2015**, *17*, 1244–1247. [CrossRef] [PubMed]
14. Wang, H.; Zhong, H.; Xu, X.; Xu, W.; Jiang, X. Catalytic enantioselective bromoaminocyclization and bromocycloetherification. *Adv. Synth. Catal.* **2020**, *362*, 5358–5362. [CrossRef]
15. Bergeron, R.J.; Xin, M.G.; Weimar, W.R.; Smith, R.E.; Wiegand, J. Significance of asymmetric sites in choosing siderophores as deferration agents. *J. Med. Chem.* **2001**, *44*, 2469–2478. [CrossRef] [PubMed]
16. Patterson, G.; Larsen, L.K.; Moore, R.E. Bioactive natural products from blue-green algae. *J. Appl. Phycol.* **1994**, *6*, 151–157. [CrossRef]
17. Ghosh, A.K.; Mathivanan, P.; Cappiello, J. C2-Symmetric chiral bis (oxazoline)–metal complexes in catalytic asymmetric synthesis. *Tetrahedron Asymmetry* **1998**, *9*, 1. [CrossRef]
18. Helmchen, G.; Pfaltz, A. Phosphinooxazolines a new class of versatile, modular P, N-ligands for asymmetric catalysis. *Acc. Chem. Res.* **2000**, *33*, 336–345. [CrossRef]
19. Meyers, A.I. Chiral oxazolines and their legacy in asymmetric carbon-carbon bond-forming reactions. *J. Org. Chem.* **2005**, *70*, 6137–6151. [CrossRef]
20. Garzan, A.; Jaganathan, A.; Salehi Marzijarani, N.; Yousefi, R.; Whitehead, D.C.; Jackson, J.E.; Borhan, B. Solvent-dependent enantiodivergence in the chlorocyclization of unsaturated carbamates. *Chem. Eur. J.* **2013**, *19*, 9015–9021. [CrossRef]
21. Jaganathan, A.; Garzan, A.; Whitehead, D.C.; Staples, R.J.; Borhan, B. A catalytic asymmetric chlorocyclization of unsaturated amides. *Angew. Chem. Int. Ed. Engl.* **2011**, *50*, 2593–2596. [CrossRef]
22. Kawato, Y.; Ono, H.; Kubota, A.; Nagao, Y.; Morita, N.; Egami, H.; Hamashima, Y. Highly enantioselective bromocyclization of allylic amides with a P/P=O double-site Lewis base catalyst. *Chem. Eur. J.* **2016**, *22*, 2127–2213. [CrossRef] [PubMed]
23. Deng, Y.; Jiang, Z.; Yao, M.; Xu, D.; Zhang, L.; Li, H.; Tang, W.; Xu, L. Palladium-catalyzed, Highly efficient, regiocontrolled Arylation of electron-rich allylamines with aryl halides. *Adv. Synth. Catal.* **2012**, *354*, 899–907. [CrossRef]
24. Hansch, C.; Leo, A.; Taft, R.W. A survey of hammett substituent constants and resonance and field parameters. *Chem. Rev.* **1991**, *91*, 165–195. [CrossRef]
25. Available online: https://en.wikipedia.org/wiki/Hammett_equation;https://organicchemistrydata.org/hansreich/resources/pka/ (accessed on 11 May 2022).
26. Chung, W.J.; Vanderwal, C.D. Stereoselective halogenation in natural product synthesis. *Angew. Chem. Int. Ed. Engl.* **2016**, *55*, 4396–4434. [CrossRef]